



# Gd<sub>3</sub>B(W,Mo)O<sub>9</sub>: Eu<sup>3+</sup> red phosphor: From structure design to photoluminescence behavior and near-UV white-LEDs performance



Shuangli Dong<sup>a</sup>, Shi Ye<sup>a,\*</sup>, Lingli Wang<sup>b</sup>, Xingyuan Chen<sup>a</sup>, Shaobei Yang<sup>a</sup>, Yujun Zhao<sup>a</sup>, Jianguo Wang<sup>c</sup>, Xiping Jing<sup>c</sup>, Qinyuan Zhang<sup>a,\*</sup>

<sup>a</sup>State Key Lab of Luminescent Materials and Devices, and Institute of Optical Communication Materials, South China University of Technology, Guangzhou 510641, PR China

<sup>b</sup>Institute of Rare Metals, Guangzhou Research Institute of Non-Ferrous Metals, Guangzhou 510650, PR China

<sup>c</sup>Beijing National Laboratory for Molecular Sciences, State Key Laboratory of Rare Earth Materials Chemistry and Applications, College of Chemistry and Molecular Engineering, Peking University, Beijing 100871, PR China

## ARTICLE INFO

### Article history:

Received 19 March 2014

Received in revised form 15 April 2014

Accepted 3 May 2014

Available online 15 May 2014

### Keywords:

Structural design

Photoluminescence performance

Tri-color phosphors

Tungstate

Molybdate

## ABSTRACT

The photoluminescence behavior of a high efficient red phosphor Gd<sub>3</sub>B(W,Mo)O<sub>9</sub>:Eu<sup>3+</sup> designed according to crystal structure and electronic structure is presented in detail. The substitution of isolated WO<sub>6</sub> group by MoO<sub>6</sub> makes the absorption band edge extend from 360 nm to 440 nm, as designed to fit the excitation of near ultraviolet (NUV) LED chip, which could be interpreted by the density functional theory calculations. The extreme low symmetry (C<sub>1</sub>) of Eu<sup>3+</sup>(Gd<sup>3+</sup>) site enables Eu<sup>3+</sup> ion to show dominant electronic dipole transition <sup>5</sup>D<sub>0</sub> → <sup>7</sup>F<sub>2</sub> (~616 nm) with five apparent splitting peaks according to group theory, which is almost 10 times stronger than that of commercial Y<sub>2</sub>O<sub>2</sub>S:Eu<sup>3+</sup> upon ~385 nm excitation. The outstanding thermal stability of photoluminescence of this phosphor up to 523 K may probably be owed to the energy transfer from isolated MoO<sub>6</sub> groups to the well-dispersed Eu<sup>3+</sup> ion separated by BO<sub>3</sub> groups. The performance of NUV white-LEDs package fabricated with a blue, green and this red phosphor is also demonstrated. It shows high color stability of the white light (CIE coordinate (0.320, 0.349), CCT 6031K, at 20 mA) under the DC drive current varied from 20 mA to 350 mA, verifying the potential application of the red phosphor in tri-color phosphors coated white-LEDs.

© 2014 Elsevier B.V. All rights reserved.

## 1. Introduction

White LEDs (w-LEDs), considered as the next generation for general lighting, have attracted much attention because of their unique advantages, for instance, high color rendering index, long lifetime, low power consumption, and environmental friendliness [1–4]. Remarkable progress has been made in the development of w-LEDs with blue LED chip coated with yellow phosphor, while for that assembled using a near ultraviolet (NUV) LED chip with tri-color phosphors, which is viewed as a more promising approach to have a better white light performance, is less investigated [3–5]. Some phosphors are selected for NUV w-LEDs application, for instance, BaMgAl<sub>10</sub>O<sub>17</sub>:Eu<sup>2+</sup> as blue phosphor, ZnS:Cu<sup>+</sup>,Al<sup>3+</sup> as green phosphor, and Y<sub>2</sub>O<sub>2</sub>S:Eu<sup>3+</sup> as red phosphor [6]. However, the red phosphor Y<sub>2</sub>O<sub>2</sub>S:Eu<sup>3+</sup> could not efficiently absorb NUV (370–400 nm) light emitted by NUV LED chip, resulting in low emission efficiency of this red phosphor and blocking the development of NUV w-LEDs [7,8]. Therefore, it is very urgent to develop new efficient red

phosphors for NUV w-LEDs [9–11]. Red phosphors with efficient absorption of the NUV light and emitting light at 610 nm are considered the best choice for a light source with respect to luminous efficiency and color rendering [8,12,13]. Recent theoretical analysis has shown that four narrow emitting sources at 459 nm, 535 nm, 573 nm, and 614 nm, respectively, are needed to obtain high luminous efficiency, high color rendering index and low correlated color temperature [14]. Particularly the red phosphor emitting 610–620 nm with FWHM less than 20 nm is highly desirable [14,15]. For this, Eu<sup>3+</sup> ion is the perfect and unique choice. Moreover, the temperature dependence of photoluminescence is also significant since it has great influence on the light output. Meanwhile, color rendering index of phosphor-coated w-LEDs is also influenced by temperature, which is a significant issue for device application since the w-LEDs devices radiate much heat [16].

Compounds with the MO<sub>x</sub> group (M is a high valence d<sub>0</sub> ion), such as vanadates, molybdates, tungstates, are widely used as hosts for Eu<sup>3+</sup>-doped red phosphors. These hosts could efficiently absorb UV light through the charge transfer state (CTS) of MO<sub>x</sub> group and easily transfer the absorbed energy to Eu<sup>3+</sup> for red emission. Tungstates widely attract people's interests due to its high melting point, excellent thermal stability and excellent

\* Corresponding authors. Tel.: +86 02087114235 (S. Ye).

E-mail addresses: [msyes@scut.edu.cn](mailto:msyes@scut.edu.cn) (S. Ye), [qyzhang@scut.edu.cn](mailto:qyzhang@scut.edu.cn) (Q. Zhang).

photoluminescence properties [17–21]. It is reported that  $\text{Eu}_3\text{BWO}_9$  borotungstate exhibits attractive red emission performance [7]. While it shows sharp line-shape excitation characteristic in the NUV region, which is not desirable for those NUV LED chips produced by different corporation or different manufacturing batches with different emitting wavelengths. The charge transfer band (CTB) of isolated  $\text{WO}_6$  group in  $\text{Eu}_3\text{BWO}_9$  locates at about 270–330 nm, and the substitution of  $\text{WO}_6$  group by  $\text{MoO}_6$  group would tune the CTB of the borotungstate to the desired NUV region as demonstrated in other cases [8,15,22–25]. To avoid the use of expensive and highly concentrated  $\text{Eu}^{3+}$  ions,  $\text{Gd}_3\text{BWO}_9$  is utilized as phosphor host. The well-defined single site of the cations ( $\text{Gd}^{3+}/\text{Eu}^{3+}, \text{B}^{3+}, \text{W}^{6+}$ ) [7,26] makes it easier to discuss the relationship between the structure and photoluminescence properties, which would open a perspective to design novel red phosphors. This work will give insight into the crystal structure–electronic structure–photoluminescence behavior of  $\text{Gd}_3\text{B(W,Mo)O}_9:\text{Eu}^{3+}$  and its performance in the fabricated w-LEDs application.

## 2. Experiment

### 2.1. Sample preparation

Nominal  $\text{Gd}_{2.94}\text{BW}_{1-x}\text{O}_9:\text{xMo}^{6+}, 0.06\text{Eu}^{3+}$  ( $x = 0-0.4$ ) and  $\text{Gd}_{3-y}\text{BW}_{0.80}\text{O}_9: 0.20\text{Mo}^{6+}, y\text{Eu}^{3+}$  ( $y = 0.06-1.20$ ) powder samples were synthesized through a high-temperature solid-state reaction technique. The starting materials were  $\text{MoO}_3$  (analytical reagent, A.R.),  $\text{Eu}_2\text{O}_3$  (99.99%),  $\text{Gd}_2\text{O}_3$  (99.99%),  $\text{WO}_3$  (A.R.) and  $\text{H}_3\text{BO}_3$  (A.R.). The stoichiometric amounts of the starting materials according to nominal formulae  $\text{Gd}_{2.94}\text{BW}_{1-x}\text{O}_9:\text{xMo}^{6+}, 0.06\text{Eu}^{3+}$  ( $x = 0-0.40$ ) and  $\text{Gd}_{3-y}\text{BW}_{0.80}\text{O}_9: 0.20\text{Mo}^{6+}, y\text{Eu}^{3+}$  ( $y = 0.06-1.20$ ) were mixed and ground thoroughly in an agate mortar. The mixture was firstly preheated at 500 °C for 5 h, then at 1100 °C for 10 h to eliminate the evaporation of  $\text{MoO}_3$ , and finally fired at 1200 °C for 10 h to form the single-phased  $\text{Gd}_3\text{B(W,Mo)O}_9$  in a muffle furnace with several intermediate grindings. In here 3 mol% excess of  $\text{H}_3\text{BO}_3$  was added as flux to accelerate the reaction.

### 2.2. Characterization

Phase identification of the obtained products were analyzed by means of a Philips PW1830 X-ray powder diffractometer (XRD) using graphite monochromator and Cu K $\alpha$  ( $\lambda = 1.54056 \text{ \AA}$ ) radiation at 40 kV and 40 mA. XRD data for refinement were collected on a Bruker D8 ADVANCE X-ray diffractometer with Cu target and Ni filter. The step-scan mode was used with setup of 40 kV  $\times$  40 mA, step 0.01°, 0.2 s/step. Rietveld refinement was conducted by TOPAS-Academic program. Diffuse reflection spectra were measured on Hitachi U-3010 spectrophotometer with  $\text{BaSO}_4$  as a reference. Theoretical calculations based on density functional theory (DFT) were conducted by the Vienna ab initio simulation package [27] with the frozen-core projector-augment-wave (PAW) method [28]. The generalized gradient approximation [29] and  $2 \times 1 \times 3k$  points were employed in the calculations. The energy cutoff of the plane wave basis was set to 450 eV. The convergence criterion for the electronic energy was  $10^{-4}$  eV and the structures were relaxed until the Hellmann–Feynman forces were less than 0.02 eV/Å. The excitation and photoluminescence (PL) spectra were recorded on the Jobin–Yvon TRIAX320 spectrometer equipped with a 450-W xenon lamp as the excitation source and a Hamamatsu R928 photomultiplier tube as detector. The temperature-dependent PL spectra were measured on the same spectrofluorimeter equipped with an additional TAP-02 High-temperature fluorescence instrument (Tian Jin Orient–KOJI instrument Co., Ltd.). Decay curves were recorded on an Edinburgh FLS920 spectrofluorometer with a  $\mu\text{F900}$  flash lamp as the excitation resource and a thermo-electronic cooled red sensitive Hamamatsu R928 photomultiplier tube as detector. NUV w-LEDs were fabricated by coating proper amounts of red phosphor of  $\text{Gd}_3\text{B(W,Mo)O}_9:\text{Eu}^{3+}$ , a green phosphor of  $\text{BaMgAl}_{10}\text{O}_{17}:\text{Eu}^{2+}, \text{Mn}^{2+}$  (Lab-prepared) [30] and a blue phosphor of alkaline earth chloroborate (Lab-prepared) [31] on an NUV LED chip ( $\sim 385 \text{ nm}$ , EP-U4545K-A3) as the primary light source. The commercial  $\text{Y}_2\text{O}_3:\text{Eu}$  phosphor (REO-1, Dalian Luminglight Co., Ltd., China) is used for the comparison with the as-prepared  $\text{Gd}_3\text{B(W,Mo)O}_9:\text{Eu}^{3+}$  phosphor. The optical properties of w-LEDs were performed by YF1000 lamp complete analysis system under a forward-bias current of 20–350 mA at room temperature (RT).

## 3. Results and discussion

### 3.1. XRD patterns and crystal structure

Some typical XRD patterns of  $\text{Gd}_{2.94}\text{BW}_{1-x}\text{O}_9:\text{xMo}^{6+}, 0.06\text{Eu}^{3+}$  ( $x = 0, 0.10, 0.20, 0.40$ ) powder samples are demonstrated in

Fig. 1. The standard card of  $\text{Gd}_3\text{BWO}_9$  (JCPDS 50-1859) is also given for comparison. The XRD pattern of  $\text{Gd}_{2.94}\text{BW}_{0.9}\text{O}_9:0.06\text{Eu}^{3+}$  sample (red curve) agrees well with the standard card of  $\text{Gd}_3\text{BWO}_9$  (black curve) in Fig. 1, indicating that the samples is single-phased and the crystal structure is not significantly changed when the dopant ions incorporate into the host. Owing to the similar radii and the same electrovalence for  $\text{Eu}^{3+}$  and  $\text{Gd}^{3+}$ , we deduce that  $\text{Eu}^{3+}$  ion substitutes for  $\text{Gd}^{3+}$  ion in the host. The XRD patterns of  $\text{Gd}_{2.94}\text{BW}_{1-x}\text{O}_9:\text{xMo}^{6+}, 0.06\text{Eu}^{3+}$  ( $x = 0.10, 0.20$ ) (magenta curve, cyan curve) powder samples are also consistent with the standard card of  $\text{Gd}_3\text{BWO}_9$  (black curve). While for the sample with high Mo content  $x = 0.4$ , additional peaks of impurity phase ( $\text{Gd}_2\text{MoO}_6$ , JCPDS file 26-0656) appear. The result suggests that the W–Mo solid solution range  $x$  in this phosphor is no larger than 0.40. To investigate the crystal structure, the Rietveld refinement of XRD pattern of  $\text{Gd}_{2.94}\text{BW}_{0.80}\text{O}_9:0.20\text{Mo}^{6+}, 0.06\text{Eu}^{3+}$  was performed (see Fig. 2), and the results are listed in Table 1. This compound has a space group of  $P6_3$ , with lattice parameters of  $a = b = 8.5571 \text{ \AA}$ ,  $c = 5.4079 \text{ \AA}$ , and cell volume of  $342.93 \text{ \AA}^3$ . Every cation has only one crystallographic site, and the Gd/Eu site has an extremely low symmetry  $C_1$ . The isolated (W/Mo) $\text{O}_6$  groups and the isolated  $\text{BO}_3$  groups with dispersive  $\text{Eu}^{3+}$  ions are arranged along  $C_6$  rotation axis ( $c$  axis), as depicted in Fig. 3.

### 3.2. Diffuse reflection spectra, electronic structure and photoluminescence behavior

Diffuse reflection spectra of  $\text{Gd}_{2.94}\text{BW}_{1-x}\text{O}_9:\text{xMo}^{6+}, 0.06\text{Eu}^{3+}$  ( $x = 0, 0.05, 0.10, 0.20, 0.25$ ) phosphors are shown in Fig. 4. It can be seen that  $\text{Gd}_{2.94}\text{BWO}_9:0.06\text{Eu}^{3+}$  has a strong absorption band in the range of 240–360 nm, which is mainly ascribed to the CTS of  $\text{WO}_6$  group [8,15,22–25]. With the increase of Mo content  $x$ , the absorption band gradually shifts to the long wavelength, reaching a maximum value of 440 nm when  $x = 0.20$ . Apparently, the redshift is owing to the CTS of  $\text{MoO}_6$  group [8,15,22–25], and the gradual redshift implies there is interaction among  $\text{MoO}_6$  groups [24]. To make better understand of this redshift, DFT calculations of electronic structure of  $\text{Gd}_3\text{BWO}_9$  and  $\text{Gd}_3\text{BW}_{0.80}\text{Mo}_{0.20}\text{O}_9$  were conducted and their band structures are depicted in Fig. 5(a) and (b), respectively. It is clear that some defect levels are formed in the band gap of  $\text{Gd}_3\text{BW}_{0.80}\text{Mo}_{0.20}\text{O}_9$  compared to that of  $\text{Gd}_3\text{BWO}_9$ , which could be responsible to the redshift shown in Fig. 4. The partial density states, as shown in Fig. 5(c), indicate that the defect bands are attributed to the incorporation of Mo, in line with the

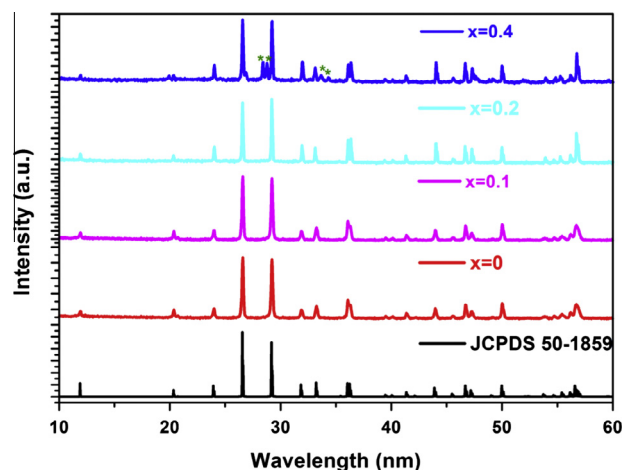
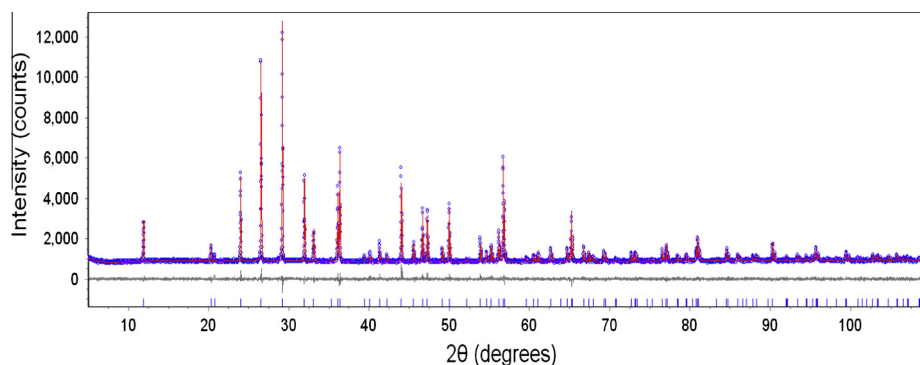


Fig. 1. XRD patterns of the  $\text{Gd}_{2.94}\text{BW}_{1-x}\text{O}_9:\text{xMo}^{6+}, 0.06\text{Eu}^{3+}$  ( $x = 0, 0.10, 0.20, 0.40$ ) series. For comparison, the standard card of  $\text{Gd}_3\text{BWO}_9$  (JCPDS 50-1859) is also presented.



**Fig. 2.** The experimental (blue dotted line) and calculated (red solid line) XRD patterns and their difference (gray solid line). (For interpretation of the references to colour in this figure legend, the reader is referred to the web version of this article.)

**Table 1**

The crystallographic data of the sample from the Rietveld refinement results.

Compounds	Gd <sub>3</sub> B(W,Mo)O <sub>9</sub>				
Space group	P6 <sub>3</sub>				
<i>a</i> (Å)	8.5570(9)				
<i>c</i> (Å)	5.4078(9)				
Cell volume (Å <sup>3</sup> )	342.93(4)				
<i>R</i> <sub>wp</sub>	3.68%				
Atoms	Wyckoff position	<i>x</i>	<i>y</i>	<i>z</i>	Site symmetry
Gd/Eu	6c	0.3579(9)	0.0828(8)	0.2118(8)	C <sub>1</sub>
W/Mo	2b	0.3333(3)	0.6666(7)	0.2500(0)	C <sub>3</sub>
B	2a	0.0000(0)	0.0000(0)	0.7800(0)	C <sub>3</sub>
O1	6c	0.1887(1)	0.0663(1)	0.8424(1)	C <sub>1</sub>
O2	6c	0.2757(4)	0.3613(8)	0.7567(8)	C <sub>1</sub>
O3	6c	0.1675(5)	0.4952(4)	0.4697(2)	C <sub>1</sub>

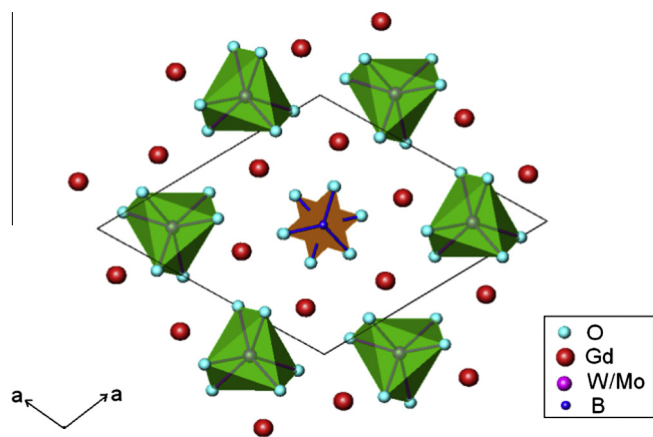


**Fig. 3.** The sketch of Gd<sub>3</sub>B(W,Mo)O<sub>9</sub> crystal structure along *c* axis.

corresponding experimental observation. Meanwhile, we found that the valence bands are dominated by oxygen while the conduction bands are mainly contributed by W/Mo (Fig. 5(c)), in line with the earlier reports that the gap is correlated to the CTS of WO<sub>6</sub> and MoO<sub>6</sub> groups [8,15,22–25].

Typical PL spectra of selected Gd<sub>2.94</sub>BW<sub>0.80</sub>O<sub>9</sub>:0.20Mo<sup>6+</sup>,0.06-Eu<sup>3+</sup> upon excitation of 385 nm light (red curve) and Gd<sub>2.94</sub>BWO<sub>9</sub>:0.06Eu<sup>3+</sup> upon excitation of 340 nm light (black curve) are described in Fig. 6(a). Emission peaks at 578, 588–598, 610–622, 650, 701–704 nm are assigned to <sup>5</sup>D<sub>0</sub> → <sup>7</sup>F<sub>*J*</sub> (*J* = 0–4) transition of the Eu<sup>3+</sup> ion, respectively. The dominant electronic dipole transition of <sup>5</sup>D<sub>0</sub> → <sup>7</sup>F<sub>2</sub> suggests that Eu<sup>3+</sup> ion locate at the site without a symmetric center, which is coincident with the crystallographic data in Table 1. According to group theory and character tables,

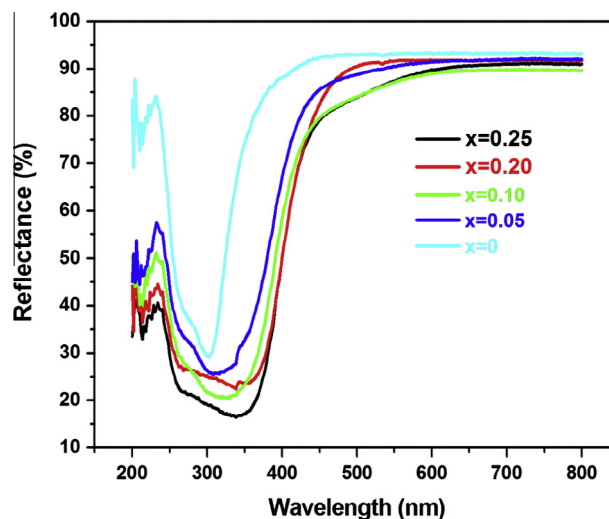


**Fig. 4.** Diffuse reflection spectra of Gd<sub>2.94</sub>BW<sub>1-x</sub>O<sub>9</sub>:xMo<sup>6+</sup>, 0.06Eu<sup>3+</sup> (*x* = 0, 0.05, 0.10, 0.20, 0.25) phosphors.

the C<sub>1</sub> symmetry of Eu<sup>3+</sup>(Gd<sup>3+</sup>) site (see the seven-coordinated polyhedron in the insert of Fig. 6(a)) would result in five splitting peaks for <sup>5</sup>D<sub>0</sub> → <sup>7</sup>F<sub>2</sub> electronic dipole transition. There are three irreducible representations (A + A + A) for electric dipole transition Hamiltonian, five irreducible representations (A + A + A + A + A) for <sup>7</sup>F<sub>2</sub> level and one irreducible representation for <sup>5</sup>D<sub>0</sub> level when Eu<sup>3+</sup> ion locates at a site with C<sub>1</sub> symmetry. Therefore, the direct product of initial state wavefunction and final state wavefunction (Ψ(<sup>5</sup>D<sub>0</sub>) | Ψ(<sup>7</sup>F<sub>2</sub>)) has five irreducible representations (A + A + A + A + A), each of which could be contained in the three irreducible

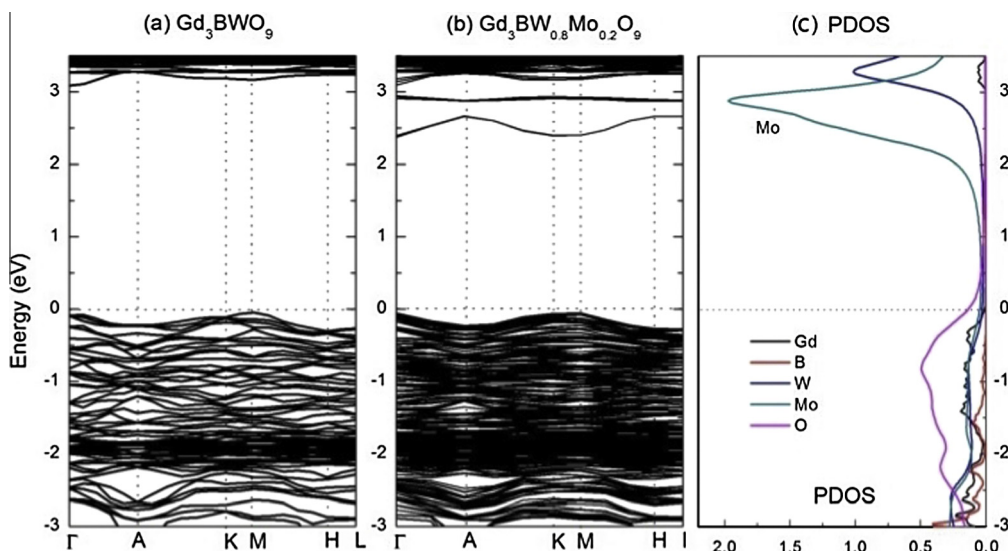


**Fig. 5.** Band structures of  $Gd_3BWO_9$  (a) and the doped system  $Gd_3BW_{0.80}Mo_{0.20}O_9$  (b), along with the projected density states (PDOS) of the doped system (c). Here the chemical ratio should be considered for the relative intensity of PDOS of the doped system since only the PDOS of one atom for each element are shown in (c).

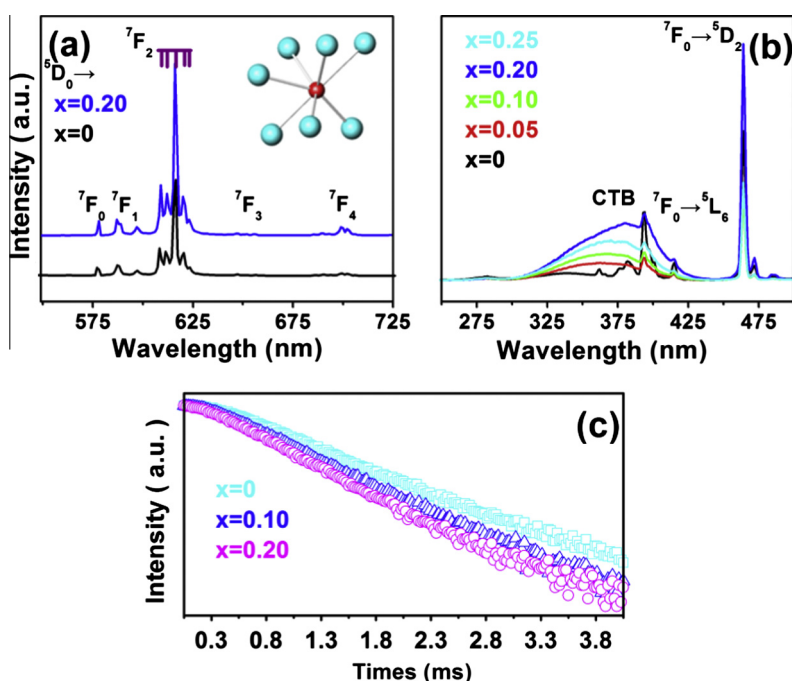


**Fig. 6.** (a) PL spectra of  $Gd_{2.94}BW_{0.80}O_9:0.20Mo^{6+}, 0.06Eu^{3+}$  sample under 385 nm excitation (red curve) and  $Gd_{2.94}BWO_9:0.06Eu^{3+}$  sample upon excitation of 340 nm light (black curve). The inset shows the  $C_1$  symmetry of  $Eu^{3+}/Gd^{3+}$  site. (b) PLE spectra monitoring 616 nm emission of  $Gd_{2.94}BW_{1-x}O_9:xMo^{6+}, 0.06Eu^{3+}$  ( $x = 0, 0.05, 0.10, 0.20, 0.25$ ) phosphors. (c) The luminescence decay curves monitoring emission at 616 nm for  $Gd_{2.94}BWO_9:0.06Eu^{3+}$  under 340 nm excitation and for  $Gd_{2.94}BW_{1-x}O_9:xMo^{6+}, 0.06Eu^{3+}$  ( $x = 0.10, 0.20$ ) upon 385 nm excitation. (For interpretation of the references to colour in this figure legend, the reader is referred to the web version of this article.)

representations  $\langle A + A + A \rangle$  of electric dipole transition Hamiltonian and thus all five splitting transition peaks are deduced theoretically. This is evidenced in Fig. 6(a) and in accordance with previous work [26]. The electronic dipole transition of  ${}^5D_0 \rightarrow {}^7F_2$  at  $\sim 616$  nm is desirable for tri-color phosphors coated NUV w-LEDs. The excitation spectra monitoring 616 nm emission of  $Gd_{2.94}BW_{1-x}O_9:xMo^{6+}, 0.06Eu^{3+}$  ( $x = 0, 0.05, 0.10, 0.20, 0.25$ ) phosphors in Fig. 6(b), are composed of a broad band and some sharp lines. For  $Gd_{2.94}BWO_9:0.06Eu^{3+}$  sample, broad excitation band locates at 240–360 nm. With the increase of Mo content ( $x$ ), the broad excitation band gradually extends to the long wavelength due to the CTB of  $MoO_6$  groups [9], which is consistent with the diffuse reflection

spectra. The broad bands originate from CTB of  $WO_6$  groups for  $Gd_{2.94}BW_{1-x}O_9:xMo^{6+}, 0.06Eu^{3+}$  ( $x = 0$ ) sample and from  $MoO_6$  groups for  $Gd_{2.94}BW_{1-x}O_9:xMo^{6+}, 0.06Eu^{3+}$  ( $x = 0.05, 0.10, 0.20, 0.25$ ) samples, manifesting that energy transfer process take place from  $WO_6/MoO_6$  groups to  $Eu^{3+}$  ions. The strong sharp lines are the characteristic intra-configurational  $4f-4f$  transitions of  $Eu^{3+}$ : 395 nm ( ${}^7F_0 \rightarrow {}^5L_6$ ) and 465 nm ( ${}^7F_0 \rightarrow {}^5D_2$ ), indicating that the low symmetry of  $Eu^{3+}$  site would break down the parity of  $f$  orbital function and result in large increase of the parity-forbidden  $4f-4f$  transition rate. The redshift is beneficial to NUV w-LEDs application because it matches well with the emitted wavelength of NUV LED chips [8]. Thus the optimum concentration for Mo in

phosphor  $\text{Gd}_{2.94}\text{BW}_{1-x}\text{O}_9:x\text{Mo}^{6+}, 0.06\text{Eu}^{3+}$  is 0.20. Fig. 6(c) presents the luminescence decay curves by monitoring emission at 616 nm for  $\text{Gd}_{2.94}\text{BW}_{1-x}\text{O}_9:x\text{Mo}^{6+}, 0.06\text{Eu}^{3+}$  ( $x = 0.10, 0.20$ ) (blue curve, magenta curve) upon 385 nm excitation and for  $\text{Gd}_{2.94}\text{BWO}_9:0.06\text{Eu}^{3+}$  under 340 nm excitation (cyan curve). The luminescence lifetime of  $\text{Gd}_{2.94}\text{BWO}_9:0.06\text{Eu}^{3+}$  phosphor is about 740  $\mu\text{s}$ , which decreases slightly with the introduction of Mo. It may be caused by some defects introduced by Mo in the lattice, which act as non-radiative relaxation centers.

Fig. 7(a) illustrates the  $\text{Eu}^{3+}$  concentration dependence of 616 nm emission intensity of  $\text{Gd}_{3-y}\text{BW}_{0.80}\text{O}_9:0.20\text{Mo}^{6+}, y\text{Eu}^{3+}$  under excitation at 385 nm. With the increase of  $\text{Eu}^{3+}$  concentration ( $y$ ), the 616 nm emission intensity increases firstly and reaches a maximum value around  $y = 0.80$ , then decreases due to the concentration quenching [32], as seen in Fig. 7(a). Thus the optimum concentration  $y$  for  $\text{Eu}^{3+}$  ion in phosphor  $\text{Gd}_{3-y}\text{BW}_{0.80}\text{O}_9:0.20\text{Mo}^{6+}, y\text{Eu}^{3+}$  is 0.80. The emission intensity of optimal phosphor is almost 10 times stronger than that of commercial  $\text{Y}_2\text{O}_2\text{S}:\text{Eu}^{3+}$  upon the excitation of  $\sim 385$  nm NUV light, as seen in Fig. 7(b). The thermal performance of phosphor is also a significant technological parameter for phosphors applied in w-LEDs [33], especially in high power devices [34]. The junction temperatures of typical LEDs can be higher than 373 K. Normally, if there is thermal quenching of a phosphor at  $T > 373$  K, emission color would shift [35]. Fig. 7(c) demonstrates the dependence of 616 nm emission intensity of  $\text{Gd}_{2.20}\text{BW}_{0.80}\text{O}_9:0.20\text{Mo}^{6+}, 0.80\text{Eu}^{3+}$  on the temperature upon 465 nm (red curve) and 385 nm (blue curve) excitation. For 465 nm excitation corresponding to the  $f-f$  transition of  $\text{Eu}^{3+}$ , the intensity almost keeps constant up to 423 K, and then decreases dramatically with the increase of temperature to 300 °C (decrease to about 60% of the initial value at 300 K when

the temperature reaches 523 K). The sharp decrease at high temperature is due to the temperature quenching effect of  $\text{Eu}^{3+}$  luminescence caused by energy migration and transfer to nonradiative traps in the host lattice [7]. While under the 385 nm excitation corresponding to the CTS of  $\text{MoO}_6$  group, the intensity could maintain constant up to 523 K. There exists energy transfer from isolated  $\text{MoO}_6$  group to the well-dispersed  $\text{Eu}^{3+}$  upon excitation at 385 nm. The energy transfer would alleviate the decrease caused by temperature quenching effect of  $\text{Eu}^{3+}$  itself. The outstanding thermal performance of the phosphor is highly desirable for NUV w-LEDs application.

### 3.3. w-LEDs performance

To evaluate the application of the red phosphor  $\text{Gd}_3\text{B(W,Mo)O}_9:\text{Eu}^{3+}$  in NUV w-LEDs, we fabricated the w-LEDs device consisting of the as-prepared red phosphor  $\text{Gd}_3\text{B(W,Mo)O}_9:\text{Eu}^{3+}$ , a chloroborate blue phosphor [31], an aluminate green phosphor [30] and a NUV LED chip (emission wavelength  $\sim 385$  nm). The photos of the above mentioned phosphors under a 365 nm UV lamp are illustrated in Fig. 8(a). Intense red, blue and green light are observed. Images of fabricated w-LEDs lamp without and with a 20 mA DC drive current are shown in Fig. 8(b) and (c), respectively. Bright white light from the LED driven by a 20 mA direct current (DC) is observed by naked eyes and the emission spectrum of the w-LEDs lamp is demonstrated in Fig. 8(d). The Commission Internationale de l'Eclairage (CIE) chromaticity coordinate of the lamp operated at 20 mA is calculated to be (0.320, 0.349), locating at the white region as depicted in Fig. 8(e). The correlated color temperature (CCT) is 6031 K, very close to that of the daylight [12].

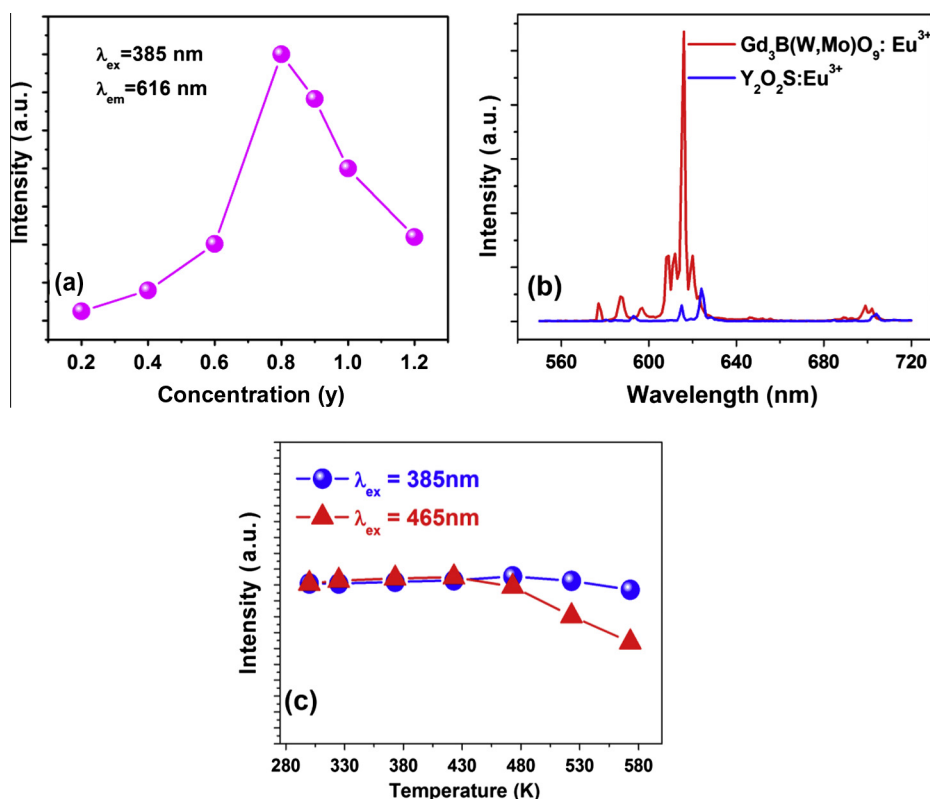
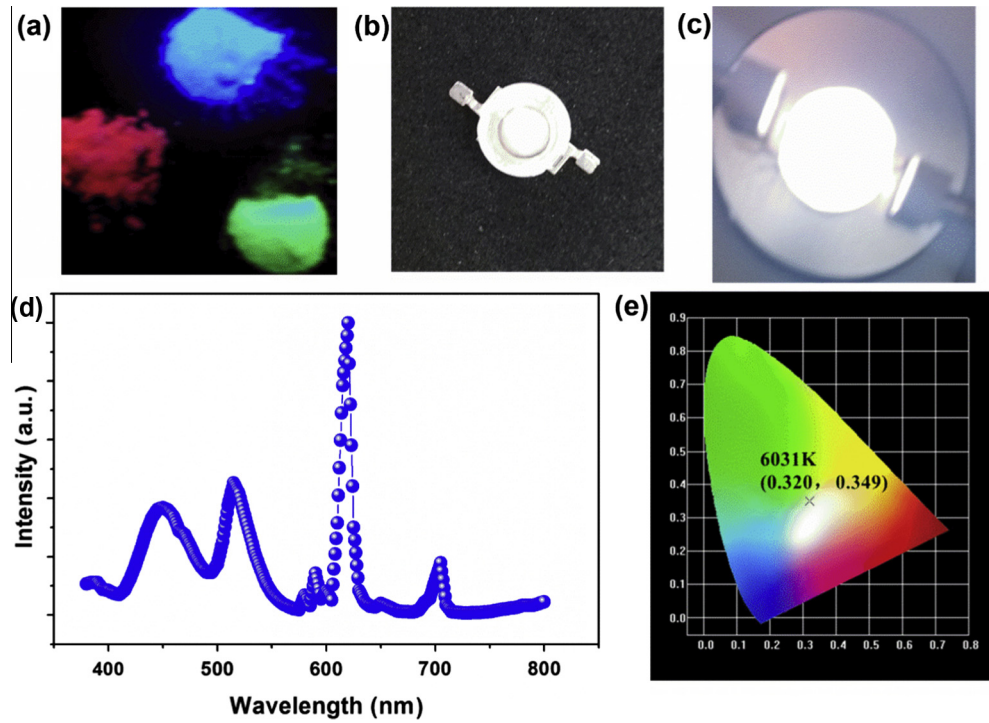
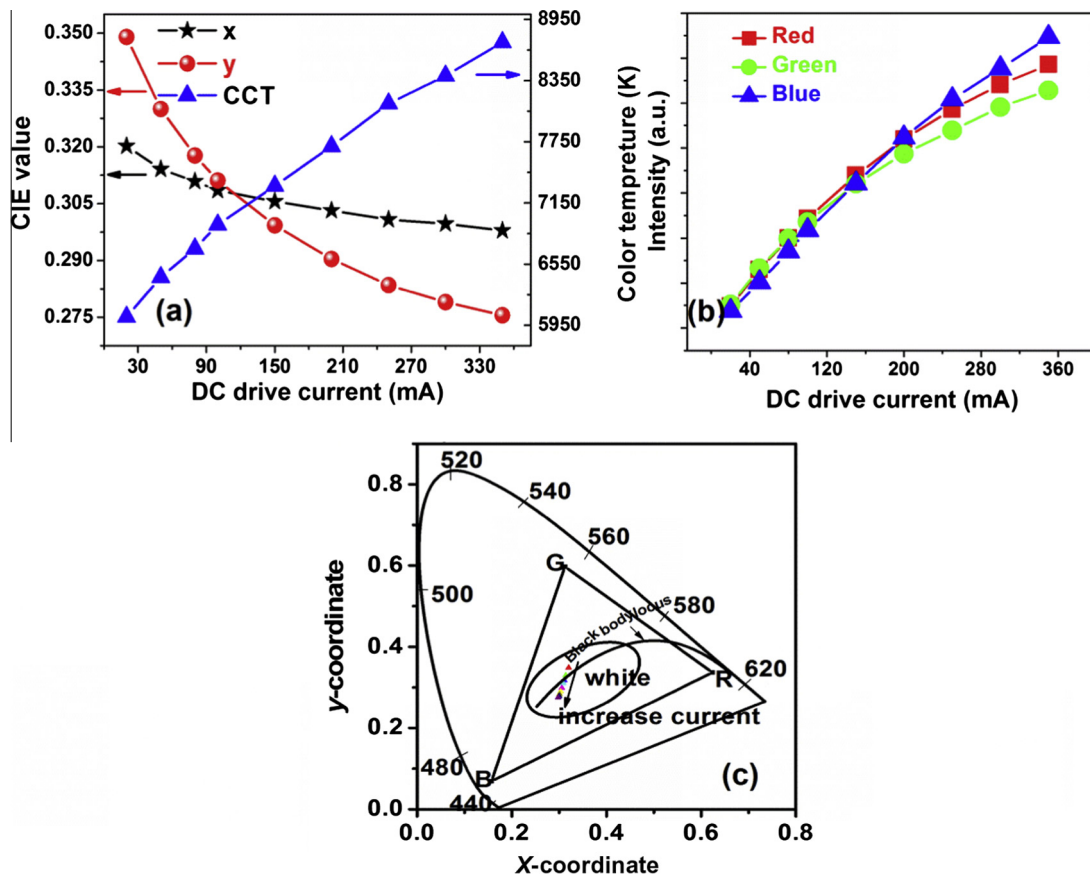


Fig. 7. (a) The dependence of 616 nm emission intensity under excitation at 385 nm for  $\text{Gd}_{3-y}\text{BW}_{0.80}\text{O}_9:0.20\text{Mo}^{6+}, y\text{Eu}^{3+}$  on the concentrations ( $y$ ) of  $\text{Eu}^{3+}$  ions. (b) PL spectra comparison between  $\text{Gd}_{2.20}\text{BW}_{0.80}\text{O}_9:0.20\text{Mo}^{6+}, 0.80\text{Eu}^{3+}$  (red curve) and commercial red phosphor  $\text{Y}_2\text{O}_2\text{S}:\text{Eu}^{3+}$  (blue curve) under excitation at 385 nm. (c) The dependence of 616 nm emission intensity under 465 nm (red curve) and 385 nm (blue curve) excitation for  $\text{Gd}_{2.20}\text{BW}_{0.80}\text{O}_9:0.20\text{Mo}^{6+}, 0.80\text{Eu}^{3+}$  on the temperature (Both data are normalized at 300 K). (For interpretation of the references to colour in this figure legend, the reader is referred to the web version of this article.)



**Fig. 8.** (a) The photos of red/blue/green phosphors under a 365 nm UV lamp. (b) Images of fabricated w-LEDs. (c) Images of fabricated w-LEDs driven by a 20 mA DC current. (d) The emission spectrum of the fabricated w-LEDs lamp operated at 20 mA. (e) The CIE chromaticity coordinates for the lamp operated at 20 mA. (For interpretation of the references to colour in this figure legend, the reader is referred to the web version of this article.)



**Fig. 9.** (a) The dependence of CIE chromaticity coordinates value (x, y) and color temperature on DC drive current. (b) The dependence of three primary colors intensities on DC drive current. (c) The variation of CIE chromaticity coordinates with different DC drive current for w-LEDs. (For interpretation of the references to colour in this figure legend, the reader is referred to the web version of this article.)

The color stability of the w-LEDs lamp under various DC drive current were performed and the results are depicted in Fig. 9. Both the chromaticity coordinate  $x$  and  $y$  decline gradually with a larger trend for  $y$ , and the CCT varies from 6031 K to 8726 K under the DC drive current varied from 20 mA to 350 mA (Fig. 9a). The integral intensities of red, green and blue component of the white light (see Fig. 8d) gradually increase with the raise of DC drive current, however, the green component (green phosphor) shows a larger saturation effect as demonstrated in Fig. 9b. In general, the chromaticity of the lamp is highly stable when the DC drive current varies in a large range from 20 mA to 350 mA, as seen in Fig. 9c, indicating that the as-prepared red phosphor is a potential candidate for tri-color phosphor-coated w-LEDs.

#### 4. Conclusions

In conclusion, we have developed a novel red phosphor  $Gd_3B(W,Mo)O_9:Eu^{3+}$  for NUV w-LEDs. The incorporation of Mo to this phosphor leads to the extension of the excitation band to the NUV region, which is ascribed to the CTS of  $MoO_6$  group and evidenced by the DFT calculations. The phosphors exhibit strong and dominant electronic dipole transition  $^5D_0 \rightarrow ^7F_2$  of  $Eu^{3+}$  with five obvious splitting peaks, which could be corresponded to the  $C_1$  site symmetry in the crystallographic data and interpreted by group theory. The integral emission intensity of the optimal phosphor is about 10 times higher than that of commercial red phosphors  $Y_2O_3:Eu^{3+}$ . The outstanding thermal stability of photoluminescence of these phosphors is probably owed to the energy transfer from isolated  $MoO_6$  groups to the well-dispersed  $Eu^{3+}$  ion separated by  $BO_3$  groups. NUV w-LEDs package is fabricated and the white light performance under various DC drive current is investigated. The research verified the potential application of the red phosphors  $Gd_3B(W,Mo)O_9:Eu^{3+}$  in tri-color phosphor coated NUV w-LEDs.

#### Acknowledgements

We gratefully thank Prof. Jing Wang for providing the  $Y_2O_3:Eu$  sample. This work is financially joint supported by the NSFC, China-(Grant Nos. 21101065, 11104266 and 51125005), and Outstanding Young Teacher Training Program of Guangdong provincial Institute of higher education (Yq2013011).

#### Reference

- [1] E.F. Schubert, J.K. Kim, Solid-state light sources getting smart, *Science* 308 (2005) 1274–1278.
- [2] Y. Kaihatsu, F. Iskandar, H. Widiyandari, W.N. Wang, K. Okuyama, Fabrication and characterization of a yellow-emitting BCNO phosphor for white light-emitting diodes, *Electrochem. Solid State Lett.* 12 (2009) J33–J36.
- [3] C.C. Lin, R.S. Liu, Advances in phosphors for light-emitting diodes, *J. Phys. Chem. Lett.* 2 (2011) 1268–1277.
- [4] S. Ye, F. Xiao, Y.X. Pan, Y.Y. Ma, Q.Y. Zhang, Phosphors in phosphor-converted white light-emitting diodes: recent advances in materials, techniques and properties, *Mater. Sci. Eng. R* 71 (2010) 1–34.
- [5] D.A. Steigerwald, J.C. Bhat, D. Collins, R.M. Fletcher, M.O. Holcomb, M.J. Ludowise, P.S. Martin, S.L. Rudaz, Illumination with solid state lighting technology, *IEEE J. Sel. Top. Quantum Electron.* 8 (2002) 310–320.
- [6] Z.L. Wang, H.B. Liang, M.L. Gong, Q. Su, A potential red-emitting phosphor for LED solid-state lighting, *Electrochem. Solid State Lett.* 8 (2005) H33–H35.
- [7] R. Zhu, Y.L. Huang, H.J. Seo, A red-emitting phosphor of Eu-based borotungstate  $Eu_3BWO_9$  for white light-emitting diodes, *J. Electrochem. Soc.* 157 (2010) H1116–H1120.
- [8] X.G. Wang, Y.L. Huang, M.Y. Young, S.L. Kim, H.J. Seo, The influence of  $Mo^{6+}$  doping on the luminescence properties of red-emitting phosphor  $Sr_9Eu_2W_{4-x}Mo_xO_{24}$  ( $x = 0-4$ ), *Ceram. Int.* 38 (2012) 4991–4995.
- [9] G. Blasse, A.F. Corsmit, Electronic and vibrational spectra of ordered perovskites, *J. Solid State Chem.* 6 (1973) 513–518.
- [10] P. He, H.H. Wang, S.G. Liu, W. Hu, J.X. Shi, G. Wang, M.L. Gong, An efficient europium(III) organic complex as red phosphor applied in LED, *J. Electrochem. Soc.* 156 (2009) E46–E49.
- [11] C.H. Chiu, C.H. Liu, S.B. Huang, T.M. Chen, Synthesis and luminescence properties of intensely red-emitting  $M_3Eu(WO_4)_{4-x}(MoO_4)_x$  ( $M = Li, Na, K$ ) phosphors, *J. Electrochem. Soc.* 155 (2008) J71–J78.
- [12] W.A. Thornton, Luminosity and color-rendering capability of white light, *J. Opt. Soc. Am.* 61 (1971) 1155–1163.
- [13] M. Koedam, J.J. Opstelten, Measurement and computer-aided optimization of spectral power distributions, *J. Light. Res. Tech.* 3 (1971) 205–210.
- [14] J.Y. Tsao, M.E. Coltrin, M.H. Crawford, J. Simmons, Solid-state lighting: an integrated human factors, technology, and economic perspective, *A. Proc. IEEE* 98 (2010) 1162–1179.
- [15] P.S. Dutta, A. Khanna,  $Eu^{3+}$  activated molybdate and tungstate based red phosphors with charge transfer band in blue region, *J. Solid State Sci. Technol.* 2 (2013) R3153–R3167.
- [16] A.A. Setlur, H.A. Comanzo, A.M. Srivastava, W.W. Beers, Spectroscopic evaluation of a white light phosphor for UV-LEDs- $Ca_2NaMg_2V_3O_{12}:Eu^{3+}$ , *J. Electrochem. Soc.* 152 (2005) H205–H208.
- [17] O. Beaury, M. Faucher, G. Teste de Sagey, P. Caro, Investigation of a new structural type for  $Y_2WO_6$ , *Mater. Res. Bull.* 13 (1978) 953–957.
- [18] F. Chevire, F. Clabau, O. Larcher, E. Orhan, F. Tessier, R. Marchand, Tunability of the optical properties in the  $Y_6(W, Mo)(O, N)_{12}$  system, *Solid State Sci.* 11 (2009) 533–536.
- [19] F. Tessier, F. Chevire, F. Munoz, C.F. Baker, O. Larcher, S. Boujday, C. Colbeau-Justin, R. Marchand, UV absorption properties of ceria-modified compositions within the fluorite-type solid solution  $CeO_2-Y_6WO_{12}$ , *J. Solid State Chem.* 179 (2006) 3184–3190.
- [20] Y. Chen, J. Wang, C.M. Liu, X.J. Kuang, Q. Su, A host sensitized reddish-orange  $Gd_2MoO_6:Sm^{3+}$  phosphor for light emitting diodes, *Appl. Phys. Lett.* 98 (2011) 081917.
- [21] Z.G. Xia, J.F. Sun, H.Y. Du, D.M. Chen, J.Y. Sun, Luminescence properties of double-perovskite  $Sr_2Ca_{1-x}Eu_xNa_xMoO_6$  red-emitting phosphors prepared by the citric acid-assisted sol-gel method, *J. Mater. Sci.* 45 (2010) 1553–1559.
- [22] H. Li, H.K. Yang, B.K. Moon, B.C. Choi, J.H. Jeong, K. Jang, H.S. Lee, S.S. Yi, Investigation of the structure and photoluminescence properties of  $Eu^{3+}$  ion-activated  $Y_6W_xMo_{(1-x)}O_{12}$ , *J. Mater. Chem.* 21 (2011) 4531–4537.
- [23] L. Zhang, Z. Lu, P.D. Han, L.X. Wang, Q.T. Zhang, Synthesis and photoluminescence of  $Eu^{3+}$ -activated double perovskite  $NaGdMg(W, Mo)O_6$  – a potential red phosphor for solid state lighting, *J. Mater. Chem. C* 1 (2013) 54–57.
- [24] S. Ye, C.H. Wang, Z.S. Liu, J. Lu, X.P. Jing, Photoluminescence and energy transfer of phosphor series  $Ba_{2-x}Sr_xCaMo_{1-y}W_yO_6:Eu, Li$  for white light UVLED applications, *Appl. Phys. B* 91 (2008) 551–557.
- [25] S. Ye, C.H. Wang, X.P. Jing, Photoluminescence and Raman spectra of double-perovskite  $Sr_2Ca(Mo/W)O_6$  with A- and B-site substitutions of  $Eu^{3+}$ , *J. Electrochem. Soc.* 155 (2008) J148–J151.
- [26] M. Maczka, P. Tomaszewski, J. Stepien-Damm, A. Majchrowski, L. Macalik, J. Hanusa, Crystal structure and vibrational properties of nonlinear  $Eu_3BWO_9$  and  $Nd_3BWO_9$  crystals, *J. Solid State Chem.* 177 (2004) 3595–3602.
- [27] G. Kresse, J. Hafner, *Ab initio* molecular dynamics for liquid metals, *J. Phys. Rev. B* 47 (1993) 558–561.
- [28] G. Kresse, D. Joubert, From ultrasoft pseudopotentials to the projector augmented-wave method, *Phys. Rev. B* 53 (1999) 1758–1775.
- [29] J.P. Perdew, K. Burke, M. Ernzerhof, Generalized gradient approximation made simple, *Phys. Rev. Lett.* 77 (1996) 3865–3868.
- [30] Chinese patent No. ZL03121541.6.
- [31] Chinese patent No. ZL200310100030.1.
- [32] X.L. Zhang, Z.S. Li, H.T. Zhang, S.X. Ouyang, Z.G. Zou, Luminescence properties of  $Sr_2ZnWO_6:Eu^{3+}$  phosphors, *J. Alloys Comp.* 469 (2009) L6–L9.
- [33] J.H. Ryu, Y.G. Park, H.S. Won, S.H. Kim, H. Suzuki, J.M. Lee, C. Yoon, M. Nazarov, D.Y. Noh, B. Tsukerblat, Luminescent properties of Ca- $\alpha$ -SiAlON: $Eu^{2+}$  phosphors synthesized by gas-pressured sintering, *J. Electrochem. Soc.* 155 (2008) J99–J104.
- [34] R.J. Xie, N. Hirasaki, Silicon-based oxynitride and nitride phosphors for white LEDs—a review, *Adv. Mater.* 8 (2007) 588–600.
- [35] M. Yu, J. Lin, Z. Wang, J. Fu, S. Wang, H.J. Zhang, Y.C. Han, Fabrication, patterning, and optical properties of nanocrystalline  $YVO_4: A$  ( $A = Eu^{3+}, Dy^{3+}, Sm^{3+}, Er^{3+}$ ) phosphor films via sol-gel soft lithography, *Chem. Mater.* 14 (2002) 2224–2231.